On the Impact of Long-Term Wave Trends on the Geometry Optimisation of Oscillating Water Column Wave Energy Converters

Alain Ulazia[a], Ganix Esnaola[b,c], Paula Serras[d], Markel Penalba[e,*]

[a]*Department of NE and Fluid Mechanics, University of the Basque Country (UPV/EHU). Otaola 29, 20600 Eibar, Spain.*
[b]*Department of NE and Fluid Mechanics, University of the Basque Country (UPV/EHU). Europa Plaza 1, 20018 Donostia, Spain.*
[c]*BEGIK Joint Research Unit (UPV/EHU-IEO) Plentziako Itsas Estazioa, University of Basque Country (UPV/EHU). Areatza Hiribidea 47, 48620 Plentzia, Spain.*
[d]*Department of NE and Fluid Mechanics, University of the Basque Country (UPV/EHU). Plaza Ingeniero Torres Quevedo 1, 48013, Bilbao, Spain.*
[e]*Department of Mechanical and Manufacturing , Mondragon University, Loramendi 4 Apdo. 23, 20500 Arrasate, Spain*

Abstract

Wave trends have been shown to be relevant to energy generation in various areas of the world. Accordingly, this article describes the impact of wave trends on the design of oscillating water column wave energy converters. First, wave trends across the North-East Atlantic Ocean are analysed based on the *ERA5* reanalysis. In addition, an empirical model that provides the capture width of an oscillating water column is employed, identifying an approximately linear relationship between the average wavelength and the optimal width of the chamber. Thus, combining wave trends and the empirical model, the optimal size of the chamber is found to vary significantly between different geographical locations and over the four decades between 1979 and 2018. Differences between the original geometry and the geometry optimised considering wave trends, reach up to 15% in some locations. As a consequence, oscillating water column chambers designed based on past available resources rather than the resource corresponding to the time when the device is to be deployed are demonstrated to be inefficient, with a significant difference in the optimal width and absorbed energy of the chamber. Accounting for changes in resource availability over time may assist in cost optimisation of unconventional renewable energy technologies.

Keywords: *ERA5*; Wave energy trends; Wave energy converters; Oscillating water column; Geometry optimisation;

List of Abbreviations

CFD	Computational fluid dynamics
OWC	Oscillating water column
CW	Capture width
CW*	Capture width ratio
PEI	Plant efficiency index
PTO	Power take off
RMSE	Root mean square error
SDratio	Standard deviation ratio
WMB	Wave measuring buoy
IPCC	International Panel for Climate Change
WEC	Wave energy converter
NWT	Numerical wave tank
ECMWF	European Centre for Medium-Range Weather Forecasting
LCOE	Levelised cost of energy
MRM	Multi-regression model

Nomenclature

H_s	Significant wave height
T_m	Mean wave period
λ	Wavelength
J_w	Wave energy flux
ω	Wave frequency
h	Water depth
k	Wavenumber
ρ_w	Water density
g	Gravitational acceleration (9.8 m/s^2)
B_{PTO}	Air-turbine induced damping coefficient
E_{abs}	Absorbed energy
W, L, T	OWC chamber width, length, and draft
P_{OWC}	OWC's absorbed power
p_{OWC}	Air pressure in the OWC chamber
q_{OWC}	Air flux in the OWC chamber
T_{sim}	Simulation time
ρ_{air}	Air density
h^*	Dimensionless water depth
W^*, L^*, T^*	Dimensionless OWC chamber width, length and draft
B^*_{PTO}	Dimensionless turbine induced damping

*Corresponding author
Email addresses: alain.ulazia@ehu.eus (Alain Ulazia), ganix.esnaola@ehu.eus (Ganix Esnaola), paula.serras@ehu.eus (Paula Serras), mpenalba@mondragon.edu (Markel Penalba)

1. Introduction

The Intergovernmental Panel for Climate Change (IPCC) has clearly stated that the effects of climate change are already noticeable, since the world is currently about 1°C warmer than in the pre-industrial era. This warming has led to the environmental alteration of approximately 75% of land and 66% of ocean areas, which is driving over a million species to extinction [1]. In addition, scientists have warned that additional increases in global temperature will significantly worsen these effects [2]. Accordingly, restricting the global temperature increase to between 1.5°C and 2°C is crucial to minimise the impacts of climate change, as agreed by 195 countries at the 2015 United Nations Climate Change Conference held in Paris [3]. To this end, the decarbonisation of the energy sector is critical, since it is responsible for the majority of greenhouse gas emissions [4].

Renewable energy production using clean energy sources such as wind, solar and hydropower, is considered to be the most promising solution to replace conventional fossil fuel plants and to transform the energy sector into a carbon-neutral system. Furthermore, an entirely renewable energy system would have important socio-economic benefits [5]. As a result, recent public policies have encouraged and stimulated the development of renewable energy generation. The European Union has become the frontrunner in shifting towards a 100% renewable energy scenario, introducing different binding renewable energy targets. These targets have been recently updated, with 20% of the final energy consumption to come from renewable sources by 2020 and 32% by 2030 [6]. Finally, the significant drop in the cost of renewable energy technologies over the last decade—mainly for solar and wind energy systems—has enabled renewable technologies to compete on the energy market with other more conventional energy technologies.

In the transition towards an entirely renewable energy system, less conventional renewable energy technologies must also contribute to the energy supply in the near future. At present, it is expected that in a partially-renewable electrified energy system that is on track to keep global temperature increases within 2°C, there will be an energy deficit that cannot be supplied by traditional renewable energy technologies by 2030 [7]. Marine renewable energy technologies are among the less conventional renewable energy technologies currently available. Some offshore wind farms were recently permitted in the North Sea, for example the 1.2 GW Dogger Bank wind farm [8], demonstrating that ocean energy can assist in the global energy transition. In addition to offshore wind, wave energy technologies—which are currently still in early development—may also be a future alternative. Currently, the cost of wave energy is too high to compete on the free market with other renewable energy technologies and the technology requires further development to close the gap between the real cost of wave energy and the market energy price. In addition, the large variety of wave energy converter (WEC) prototypes, including the absorber and power take-off (PTO) systems [9], complicates the convergence towards a successful and commercially viable technology. WECs have been already designed for multiple alternative purposes, some of which are closely related to climate change mitigation, including desalination [10], coastal protection [11] and flooding mitigation [12].

Regardless of the application for which a WEC is designed, the optimisation of the WEC's geometry is essential to minimise cost of production while maximising energy absorption capacity. To design a WEC effectively by model-based optimisation, several aspects should be considered. First, the wave energy resources (*e.g.* wave conditions and bathymetry) should be adequately characterised at the target location, since different WEC design concepts may be more suitable depending on the wave resources available [13, 14]. Furthermore, the performance of the WEC should be accurately recapitulated, i.e. the mathematical models should incorporate all relevant features and information regarding the WEC, including nonlinear dynamics when required [15, 16]. Moreover, control strategies should be integrated in the geometry-optimisation algorithm [17, 18]. However, optimisation requires computationally efficient mathematical models, which may be in conflict with the need for high-fidelity models that incorporate an effective controller.

Several previous studies have analysed the challenges of geometry optimisation for different WEC designs. The optimal geometry of point absorber WECs is analysed in [19] and the optimal sizing of the Corpower device is studied using a techno-economic model that supports the design decisions considering the performance and cost of the WEC. A cost-optimised design for a heaving point absorber WEC is also suggested in [20], for wave resources that were evaluated in the Mediterranean Sea. In contrast, geometry optimisation of bottom-hinged oscillating surge WECs is discussed in [21] and [22], where only the hydrodynamic performances of the WECs were evaluated . Other studies, such as [23], [24] and [18], have also suggested methodologies to optimise the geometry of point absorber WECs, considering only hydrodynamic performance. In [24], the shape and dimensions of the WEC hull were optimised using an impedance-matching control strategy. Notably, [18] demonstrates that including energy-maximising control strategies significantly affects the geometry optimisation of the WEC. Similarly, geometry optimisation of oscillating water column (OWC) WECs has been discussed in the literature, for both fixed and floating devices. The ratio between the side-length and the depth of a fixed OWC chamber was optimised in [25], where a fully nonlinear computational fluid dynamics (CFD)-based numerical wave tank (NWT) was used. Furthermore, the UGEN floating OWC device was optimised in [26].

The aforementioned studies all used numerical solutions based on the simplified governing flow equations for WEC geometry optimisation. In contrast, [27] presents an em-

pirical model to support the optimisation of the main design parameters of fixed OWC devices. The formulation of the empirical model was developed using an extensive dataset obtained through experimental testing and CFD simulations. The empirical model suggested in [27] predicts the capture width (*i.e.* the hydrodynamic performance) of fixed OWCs and considers the effects of nonlinear phenomena. This model thus successfully integrates two of the main requirements for mathematical models to be effectively used for optimisation as the model is high-fidelity and has a low computational cost.

Some previous geometry optimisation studies consider realistic wave climates by evaluating different geographical locations, and illustrate the impact of available wave resources on the optimal geometry of WECs [19]. However, to the best of our knowledge, no study to date has shown the impact of wave trends on the optimal geometry of WECs. Hence, all geometry optimisation strategies presented in the literature have used past data for wave resources to optimise WECs which will be deployed in the future. Importantly, wave trends have been demonstrated to have significant impacts on wave resources available in some areas of the world. Important positive wave trends in the Bay of Biscay, off the west coast of Ireland, and the Chilean coast have been demonstrated in [28], [29] and [30], respectively. In these areas, an increase in mean wave energy and a significant increase in the frequency of extreme weather and wave events has been observed. Therefore, the empirical model proposed in [27]—further described in Section 2.2.2—is used in this study to analyse the impact of wave trends on the optimal geometry of a fixed OWC device.

The remainder of this paper is organized as follows: Section 2 introduces the area of study and the wave resource data used in the analysis. It also describes the OWC device and the empirical model used in the optimisation. Section 3 presents the results of the optimisation, showing the variations of the optimal OWC chamber for different geographical locations and time periods. In Section 4, some of these results are discussed and finally, Section 5 describes the most significant conclusions of this study.

2. Data and Methodology

2.1. Wave Energy Resource

The wave resources of a particular location are dependent on several large-scale and small-scale factors such as the characteristics of the underlying continental shelf and the bathymetry of the location, the soil composition of the seabed, and the characteristics of prevailing ocean fetches and winds in the area. These factors vary significantly both geographically and in time, producing remarkable differences in wave resources between different geographical points and over time. The impact of both geographical and temporal wave resource variations on the optimal geometry of an OWC WEC are analysed in the present work.

This study considered the wave resources of an extensive geographical area over a broad period of time. In particular, we examined the North-East Atlantic Ocean, from 20° to 60° in latitude and from -20° to 0° in longitude, as illustrated in Figure 1, from 1979 to 2018.

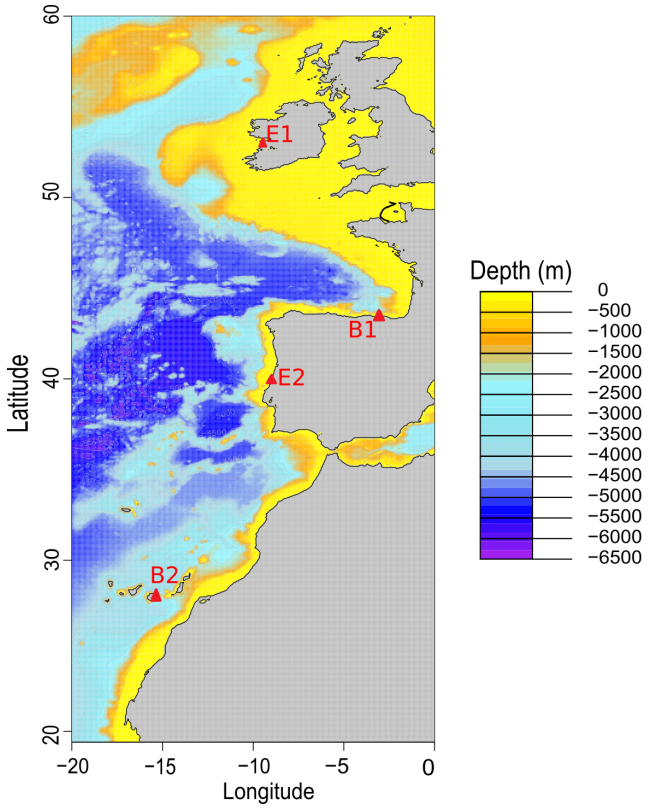

Figure 1: Area of study and the bathymetry map with the four highlighted locations: Zierbena (B1), Las Palmas (B2), Galway (E1), and Leiria (E2).

For the analysis of wave energy resources, four parameters were analysed: the significant wave height (H_s), the mean wave period (T_m), the wavelength (λ) and the wave energy potential (J_w). Variations of these four parameters were analysed over the whole area of study for the preiod from 1979 to 2018. H_s and T_m can be directly measured using wave-measuring buoys (WMBs) or can be obtained by reanalysis of existing data. However, the remainder of the variables were computed by combining wave height and period (or frequency ω), and water-depth (h) using the dispersion relation [31].

Based on the bathymetry data over the area of study shown in Figure 1, the wave energy resource parameters were combined by applying the appropriate simplifications to determine the wave energy potential in deep, intermediate and shallow waters as follows:

$$J_w = \frac{1}{16}\rho_w g H_s^2 \frac{\omega}{k}\left(1+\frac{2kh}{\sinh(2kh)}\right)\left(1+\frac{9}{64}\frac{H_s^2}{k^4h^6}\right) \quad (1)$$

where k is the wavenumber, g is the acceleration due to gravity and ρ_w is the water density.

2.1.1. Wave data: Reanalyses and Observations

To represent the vast geographical area illustrated in Figure 1 efficiently, climate reanalyses produced by the *European Centre for Medium-Range Weather Forecasts* (ECMWF) combining past observations with models were a valuable source of data. The ECMWF offers a variety of different reanalyses, from the *ERA20C* that covers the whole 20$^{\text{th}}$ century from 1900 to 2010, to the newest version *ERA5* that will cover the period from 1950 to the present with increased data frequency and spatial resolution (hourly and every 30 km, respectively). The *ERA5* reanalysis has been proven to perform better than previous reanalyses [32], which is why it was chosen for this study. Additionally, to improve the robustness of the analysis, the data generated from the *ERA5* reanalysis were validated against in-situ buoy measurements collected from two specific locations in the North-East Atlantic Ocean (see Figure 1):

B1: *Zierbena*, located within the inner Bay of Biscay [33], and

B2: *Las Palmas*, deployed in the Canary Islands, more specifically, in the eastern region of the Gran Canaria Island [33].

Further details of the two WMBs are provided in Table 1. For a specific location, the data corresponding to the nearest ERA5 gridpoint were considered for the computation of wave trends and to evaluate the historical evolution of the optimal OWC size. In the case of *B1*, the closest gridpoint is centred north of the buoy location at (3.0°W, 43.5°N). *B2* falls on the land mask of the grid (due to the characterization of the sea/land frontier using a 30 km spatial grid), so the closest *ERA5* gridpoint to the east of the buoy at (15.0°W, 28.0°N) was selected. Furthermore, two extra *ERA5* gridpoints—*E1* and *E2*—were selected close to Ireland and Portugal, respectively (see Figure 1):

E1: *Galway Bay*, using the *ERA5* gridpoint at (9.5°W, 53°N), where the water depth is approximately 52 m, and

E2: *Vieira de Leiria*, for which the coordinates of the *ERA5* gridpoint are (9°W, 40°N) with an approximate water depth of 35 m.

The validation of the E1 and E2 gridpoints was not considered in this paper, but was previously described in [34] and [35], respectively.

The specific selection of the four locations was justified using the empirical method employed in this study, further described in Section 2.2.2. Of note, this method is limited to a defined range of water depth/wavelength ratios defined in Equation (2), referred to as the dimensionless water depth (h^*), as follows:

$$h^* = kh = 2\pi h/\lambda. \tag{2}$$

In addition to the four specific locations described above, the optimal dimensions of the OWC chamber were considered for the whole area of study, with the exception of those areas that did not fulfill the requirements of the empirical approach.

Table 1: Main characteristics of the wave-measuring buoys

Buoy	*B1*	*B2*
Location (lon, lat)	Zierbena (3.07°W, 43.37°N)	Las Palmas (15.39°W, 28.05°N)
Water depth [m]	22	30
Data period	2001-2019	1992-2019
Nearest gridpoint	(3°W, 43.5°N)	(15°W, 28°N)
Validation period	2001-2018	1992-2018

However, the dimensionless water depth of the study area can only be defined once the wavelength at the location is determined (see Equation 2). This determination is challenging as the wavelength, which depends on the wave period, varies significantly across the North-East Atlantic Ocean over the course of the 20$^{\text{th}}$ century, as demonstrated in previous studies [28, 34, 35, 36]. Therefore, the area where the empirical model is valid varies in time and could not be predefined before carrying out the study.

The average wave energy resource parameters over the area of study between 1979 and 2018 are shown in Figures 2 (a), (b), (c) and (d), illustrating H_s, T_m, λ and J_w, respectively.

2.1.2. Wave Data Validation

Data from the ECMWF reanalyses have been previously validated against wave observations measured using WMBs from different locations around the world, with satisfactory results. Previous validation has been performed using wave observations from the west coast of Ireland [34], the Bay of Biscay [28], the south coast of Iceland [36], three different points along the Chilean coast [30], and off the west coast of Brittany and Galicia [35]. However, it should be noted that all locations considered in previous studies are deep-water locations, while the WMBs described in Table 1 are located in intermediate-waters. Thus, *ERA5* reanalysis wave data required additional validation for the intermediate-water locations described here.

To this end, the *ERA5* data were compared to the data collected via the WMBs. Since the most critical parameter for the optimisation of an OWC chamber is the wave period, T_m was used as the parameter for validation. Observed and reanalysed data were compared for the validation periods outlined in Table 1, for each WMB. The comparison was performed using three statistical metrics: the Root Mean Square Error (RMSE), the Pearson correlation coefficient, and the standard deviation ratio (SDratio) between the model and the buoy observations. These three metrics can be graphically illustrated together using

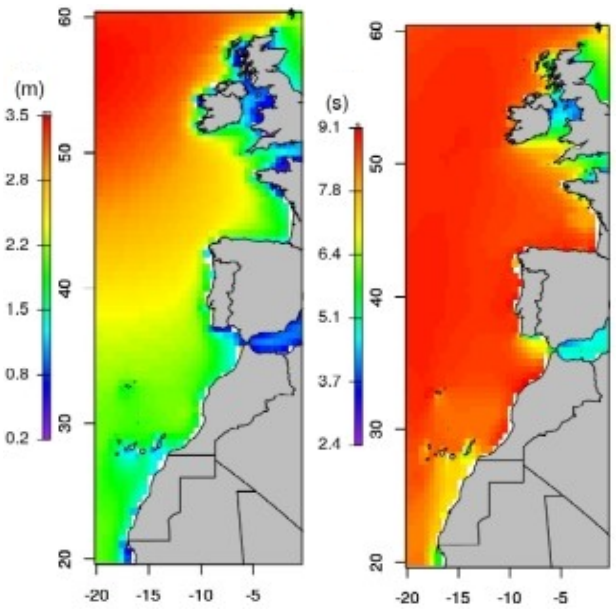

(a) Significant wave height (b) Mean wave period

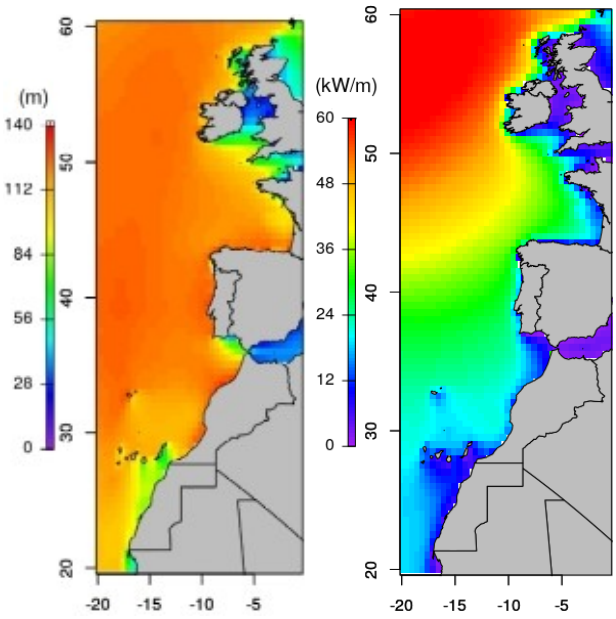

(c) Wavelength (d) Wave energy potential

Figure 2: Wave energy resources of the North-East Atlantic Ocean: (a) mean H_s, (b) T_m, (c) λ, and (d) J_w

Taylor diagrams [37], where

1. the RMSE is given by the radius of the arc centred at the point corresponding to the observation,
2. the Pearson correlation coefficient is represented by the angular position of the analysed point over the exterior arc, and
3. the SDratio is represented by the origin centred radius of the arc.

The results of the T_m validation for Zierbena and Las Palmas are illustrated in Figures 3 (a) and (b), respectively. Good agreement between the model and WMB measurements was observed for Zierbena, with correlation coefficient greater than 0.7. In contrast, the agreement between the WMB and the *ERA5* reanalysis for Las Palmas is modest, with a low correlation coefficient of approximately 0.4 . The low correlation can be attributed to the relative locations of the buoy and the model gridpoint. The buoy is close to the coast to its west and north , which means that the buoy is sheltered from swells coming from the northwest and the north—the predominant directions of the swells in *Las Palmas*. In contrast, because the *ERA5* grid point is not as sheltered by the coast, the swells from the north and northwest have a greater impact on the reanalysis data. When the winter and summer periods were evaluated separately, the correlation coefficient increased significantly for the summer period, reaching as high as 0.8 in certain months. This indicates that the major differences between WMB-measured data and model outputs are likely due to the different processes affecting their respective locations, rather than a lack of precision in the reanalysis process. With regards to the other metrics, the RMSE and SDratio are similar for both locations, with an RMSE greater than 1.5 s and a variability of greater than 1.5 times the buoy signal's SD. Hence, despite the poorer results obtained for Las Palmas, the data from the closest gridpoint in *ERA5* were considered accurate for both locations.

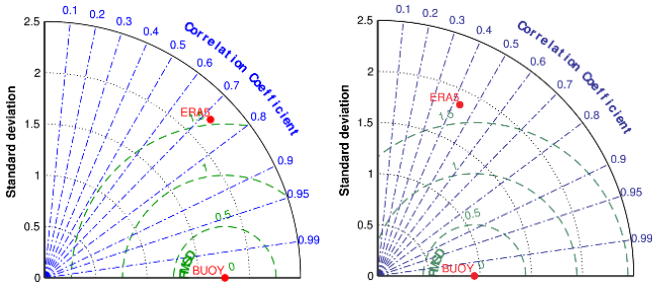

(a) Zierbena (b) Las Palmas

Figure 3: Taylor diagrams for T_m: *ERA5* versus buoys at Zierbena and Las Palmas

2.2. Oscillating Water Column

Among the existing technologies to harvest energy from ocean waves, the OWC is one of the simplest and most successful concepts. An OWC device consists of a fixed or floating structure with an internal chamber that is partially filled with water from the bottom, which generates a water column within the structure. Ocean waves induce the motion of this water column, which in turn drives air flow in and out the chamber through an air turbine that is usually located at the top of the chamber. The bidirectional air flow drives the air turbine, which is coupled to an electric generator . Further information about OWC devices can be found in [38, 39].

Fixed OWCs have been installed in coastal environments or integrated in breakwaters. Two examples of fixed-OWC plants are the Pico Plant in the Azores (Portugal) built in 1999 [40], and the LIMPET plant on the island of Islay (Scotland) constructed in 2000 [41]. Similar to these two plants, 16 chambers with a total of 16 air turbines were integrated into the breakwater constructed in the harbour of Mutriku in 2008 [42]. Floating OWC devices have also been tested in open ocean. The full-size, 1.25 MW OE-Buoy from the Irish company Ocean Energy, originally known as the Backward Bent Duct Buoy [43], is currently about to be tested in Hawaii. Other smaller scale devices, such as the Mk3 device from Oceanlinx [9], the Mighty Whale developed by the Japan Marine Science and Technology Center [44], and the MARMOK-A-5 developed by IDOM-Oceantec [45], have also been tested in open ocean waters.

The power absorption capability of OWC devices is usually evaluated by the device's pneumatic power, as per Equation (3), where the dynamics and losses/efficiencies of the air-turbine and the electric generator are ignored.

$$P_{OWC} = \frac{1}{T_{sim}} \int_0^{T_{sim}} p_{OWC} \cdot q_{OWC} dt, \tag{3}$$

where T_{sim} is the period of time over which the performance of the OWC device is being evaluated, p_{OWC} is the air pressure in the OWC chamber and q_{OWC} is the air flux in the chamber.

However, the hydrodynamic performance of WECs, regardless of the principles used to harvest energy from ocean waves, is often evaluated using the capture width (CW) [46, 35], which is defined as follows:

$$CW = \frac{P_{OWC}}{J_w}. \tag{4}$$

Based on this equation, the hydrodynamic performance of any WEC can be given as a length unit that defines the width of the wavefront (assuming uni-directional waves) with the same amount of power as that absorbed by the WEC. Another way to illustrate the performance of a WEC is by the capture width ratio (CW^*), which is given by normalising the CW to the characteristic length of the WEC.

In the specific case of the OWC studied in this work, the characteristic length is the width of the OWC chamber W (see Figure 4). Finally, the normalised capture width ratio can also be given as a percentage illustrating the hydrodynamic efficiency of the WEC [46].

2.2.1. Chamber geometry Definition

The chambers of most of the abovementioned existing OWC devices, either fixed or floating, are rectangular, except for the MARMOK-A-5, which has an axisymmetric chamber. Hence, the optimisation of an OWC device with a rectangular chamber is a practical exercise with direct implications for real OWC prototypes. The most relevant dimensions of a rectangular OWC chamber are illustrated in Figure 4, where W is the width, L is the length, h is the water-depth and T is the draft of the front wall. It should be noted that the nomenclature used here for the empirical model is slightly modified from the original study [27].

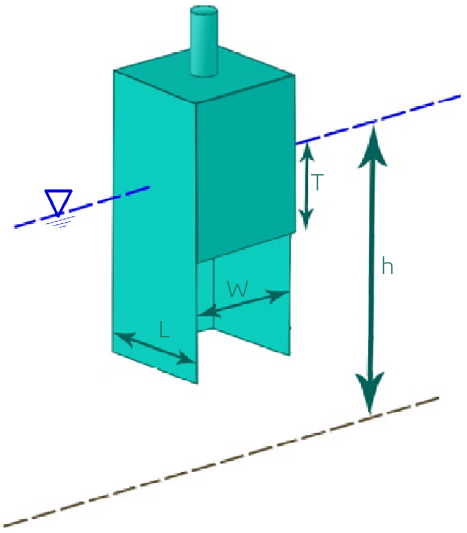

Figure 4: Most important geometric parameters of the rectangular OWC chamber.

In the present study, similar to the original study [27], the length L and width W of the chamber were forced to be identical ($L = W$). In addition, the draft of the front wall of the chamber T was kept constant for simplicity. Finally, the water-depth h was considered constant for each investigated location, and only varied by location according to the bathymetry of each point, as illustrated in Figure 1.

2.2.2. Empirical Model

The model employed in this study to predict the performance of the OWC described in Section 2.2.1, was originally proposed in [27]; thus, only a brief summary of the model is presented in this section. For further details about the empirical model, the reader is referred to the original study, where the model is thoroughly described.

The empirical model was developed using a Multi-Regression Model (MRM) based on laboratory experiments [47] and CFD simulations [48]. The model describes the dependence of OWC performance (as indicated by the capture width ratio) on the incident wave parameters (H_w, k and h), OWC chamber geometry parameters (W, L, T), turbine-induced damping (B_{PTO}) and fluid properties (ρ_w and air density ρ_{air}). Given the large number of independent variables, a group of *ad hoc* dimensionless parameters were created using the Π-*theorem*; these parameters are h^*, W^*, L^*, T^* and B^*_{PTO}. The capture width ratio can be expressed as a function of these dimensionless parameters:

$$CW^* = f(h^*, W^*, L^*, T^*, B^*_{PTO}), \tag{5}$$

for which the function f is defined as,

$$CW^* = \frac{f_1\left(K^3 - d\left(h^*\right)\right)}{f_2\left(B^*_{PTO}\right) \cdot f_3\left(W^*\right) \cdot c\left(h^*\right)}, \tag{6}$$

and the sub-functions are given as follows:

$$f_1\left(K^x - d\right) = \frac{\left(p_1\left(K^* - d\right)\left(P_2\right)\right.}{\left(\left(K^* - d\right)^2 + Q_1\left(K^* - d\right) + Q_2\right)}, \tag{7}$$

$$f_2\left(B^*_{PTO}\right) = \exp\left(a\left(h^*\right) B^*_{PTO}\right), \tag{8}$$

$$f_3\left(W^*\right) = 1 + \left(W^* - W^*_{\text{opt}}\right)^2 \cdot b\left(h^*\right). \tag{9}$$

To consider nonlinear phenomena observed in the laboratory experiments and numerical simulations, the empirical model was fitted with a relatively high-order polynomial. In addition, given the difficulty of accurately predicting the performance of an OWC device for a wide range of parameters, the MRM was formulated to ensure the highest accuracy for the range of parameters for which the greatest CW^* is expected. This empirical model was validated against experimental results that were not used in the creation of the model, showing an overall R^2 value of 0.95, a RMSE of approximately 0.053, and a maximum absolute error of approximately 0.2 with 92% of the cases having an absolute error less than 0.15.

2.2.3. Geometry Optimisation Procedure

The optimisation of the OWC chamber was considered over a wide geographical area and time period to evaluate the impact of long-term resource variations on the optimal OWC chamber geometry. The main objective of the study was to determine whether these long-term resource variations, particularly the decadal wave trends that have been observed in previous studies [28, 34, 30, 35], affects the optimal design of WECs. To this end, the optimisation of all the geometric parameters was not necessary; thus, some of the parameters were kept constant. Table 2 summarizes the value of each geometric parameter and the turbine-induced damping (B_{PTO}), providing a single value for the parameters that were kept constant and a range of values for those that were included in the optimisation algorithm.

Table 2: Main parameters of the optimisation process.

Parameter	**Value**
h^*	*Intermediate-depth*: 1.5:3.5
L [m]	7:0.2:14
W [m]	7:0.2:14
T [m]	3.5
B_{PTO} [Ns/m]	$6{:}14{\times}10^{-1}$

Table 2 also presents the range of h^* for which the empirical model described in Section 2.2.2 is valid. The dimensionless water-depth was computed at each gridpoint of the study area at different periods between 1979-2018 to assess whether the empirical model is valid for each gridpoint and time period. Therefore, the water depth is a constant in the optimisation process. As a consequence, the optimisation procedure used here was a two-parameter optimisation that evaluated the optimal size of the chamber walls W_{opt} and the optimal turbine-induced damping coefficient B_{PTO} as a function of the wave energy resources at each location and time.

The parameter ranges shown in Table 2 were defined to satisfy the requirements of the empirical model proposed in [27]. The main limitation of this approach is the dimensionless water depth h^*, which can only vary between 1.5 and 3.5 for the empirical model to be sufficiently accurate to draw meaningful conclusions. The width W and length L of the OWC chamber were always equal ($W = L$) and varied between 7 and 14 m. In contrast, the front-wall draft T was kept constant in the optimisation, using the reference value of 3.5 m given in [27]. Finally, a set of turbine-induced damping values B_{PTO} was defined for the optimisation, ensuring that the optimal values were within the permitted range.

3. Results

The optimal dimension of the OWC chamber was evaluated over the whole study area in the North-East Atlantic Ocean for the four decades between 1979 and 2018. Therefore, an accurate assessment of the wave resources was necessary. Figure 2 illustrates the average values of the wave parameters during the four studied decades, but the evolution of the resources during this time is more significant for the optimisation of the OWC chamber. Thus, wave trends in the study area are described in Section 3.1, and the impact of these trends is evaluated in Section 3.2. The impact of spatial and temporal resource variations on the OWC chamber optimisation are described separately.

3.1. Long-Term Wave Trends

An initial analysis of the wave trends in the North-East Atlantic Ocean for the whole study area was performed using the *ERA5* reanalysis, primarily relying on the wavelength λ. The vast majority of the study area corresponds to deep-water areas, where significant positive wave trends are found. Figures 5 (a) and (b) illustrate the average wavelength for the first (1979-88) and last (2009-2018) decades of the study period, respectively, highlighting the positive wave trends of the wave resources in deep-water areas.

In deep-water areas, the average wavelength increased from approximately 120 m in the first decade (1979-88) to 130-140 m in the last decade (2009-18), which corresponds to an increase of more than 10% over four decades. With regards to the intermediate- and shallow-water areas, which are particularly relevant in the present study, the effective representation of wave trends in Figure 5 for

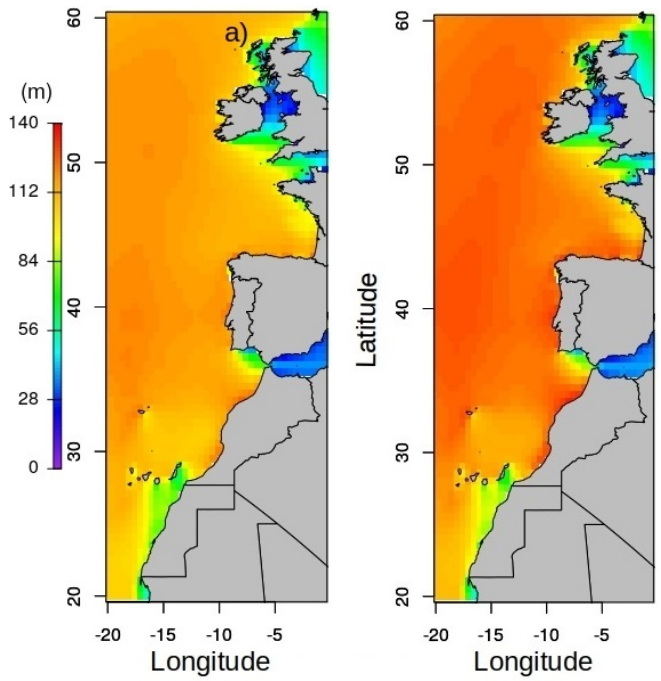

(a) λ (m) - 1979-88 (b) λ (m) - 2009-18

Figure 5: Average wavelength λ in the first and last decades of the study period: (a) 1979–1988, (b) 2009–2018.

these regions is difficult due to the large study area and the relatively small area of the intermediate- and shallow-water regions. Therefore, the information related to these regions is shown in Table 3, where data from the *ERA5* reanalysis were used for the four points B1, B2, E1, and E2. In addition, the trends for each decade were non-linear and were c omputed using the *Theil-Sen* method [49] and are expressed by percentage values with respect to the average wavelength of the entire period P=[1979-2018], $\overline{\lambda}_P$. Hence, the decadal increase in percentage $\Delta\lambda(\%)$ is given as follows,

$$\Delta\lambda(\%) = \frac{m \cdot 12 \cdot 10}{\overline{\lambda}_P} \times 100 \qquad (10)$$

where m is the mean monthly slope of λ within the corresponding decade.

Table 3: Wave trends as a percentage for selected intermediate-water depth regions for λ.

$\Delta\lambda(\%)$	1979-88	1989-1998	1999-2008	2009-18
B1	0.0	-7.2	-6.9	+14.3
B2	-4.1	+5.2	-10.5	-0.6
E1	-1.4	-4.9	-5.2	+4.6
E2	-0.8	-0.9	-4.1	+5.6

The table shows very strong positive wave trends for the final decade, particularly for E1, E2 and B1, in Galway, Leiria and Zierbena, respectively. However, there are also reductions in the second and third decades. Las Palmas (B2) also shows negative and positive trends, but a strong reduction in the third decade establishes a generally negative trend in this location. Therefore, for intermediate waters near the coast, it cannot be concluded that there is a consistent positive trend over 40 years as is the case for the studied deep water regions.

Figure 6 illustrates the previous trends at the four locations for the monthly evolution of the normalised λ with respect to the average historical value, where the slopes corresponding to each decade are plotted using green solid lines. It can be seen that at Galway and Leiria—the locations that are more exposed to the open ocean—there are correlated patterns over the four decades, without a clear trend in the first decade, reductions in the second and third decades, and an increase in the final decade. This decadal pattern is very similar in the Bay of Biscay (*B1*), but the reductions and the final increase in 2009-2018 are more significant. In contrast, the trends in Las Palmas (*B2*) show a different pattern with negative trends in the third decade, but without the important positive trends in the other decades. It should be noted that the reference for computing the slope in each decade was the 40-year average and that the trend calculation was independent of the previous or following decades.

The wave trends shown in Figure 6 are consistent with the results shown in Figure 5. The reduction in the first decade and the substantial increase in the final decade create a general positive trend over the 40-year period when the last and the first decades are compared.

3.2. Geometry Optimisation

The wavelength (directly related to the wave period) is the most relevant resource parameter in the design of an OWC chamber; thus, due to the significant variation of the average wavelength over the four decades considered, a reasonable variation of the optimal OWC chamber dimensions is to be expected. Figures 7 (a), (b) and (c) represent the CW^* of the OWC chamber as a function of the chamber width W and the turbine-induced damping B_{PTO} for wavelengths of λ =70 m, λ =90 m and λ =110 m, respectively. A maximum CW^* point can be easily identified for the three considered wavelengths, which demonstrates that the optimisation ranges defined in Table 2 are adequate. Hence, these centres provide the optimal (W,B_{PTO}) couple, which shows the relevance of control in the optimisation of the OWC chamber dimensions.

Apart from the three wavelengths illustrated in Figure 7, optimisation was conducted by a discrete optimisation approach, where wavelengths between 60 and 120 m were analysed using a step-size of 1 m. Hence, the optimal dimension of the OWC chamber can be represented as a function of the wavelength, as illustrated in Figure 8, where the optimal width increases almost linearly with the wavelength. The optimal width W approximately doubles from 8 to 14 m between the 60 m and 120 m wavelengths. These limits, illustrated by blue vertical lines in Figure 8,

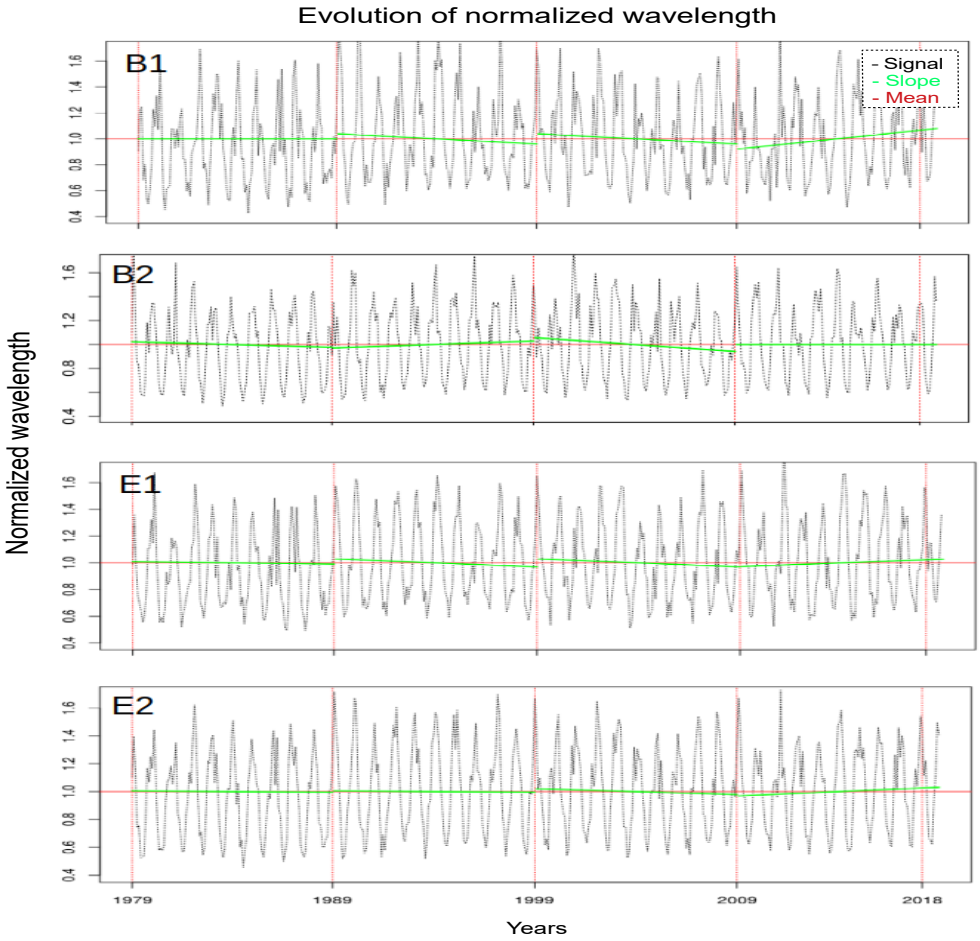

Figure 6: Monthly time series of the normalised λ over the four studied decades and the corresponding slopes of the trends for each decade (green). The average wavelength over the entire period is the normalisation factor at 1 plotted with a red horizontal line.

are established by the valid range of the empirical model proposed in [27].

The four locations described in Section 2.1.1 are included in the range established in Figure 8. The only critical location may be *B2* in Las Palmas, which presents the longest λ values, with an average of λ of approximately 120 m, which is near the upper limit of the application range for the empirical model. The average values of λ at the other three locations are between 95 m and 103 m, indicating that the model is suitable for parameter optimisation at these locations.

3.2.1. Impact of Geographical Location

Geographical variations in the wave energy resources are illustrated in Figure 2, where significant differences are evident between the different locations in the North-East Atlantic Ocean. Since wavelength is the most relevant resource parameter for OWC WEC design, particular attention should be paid to Figure 2 (c). The average wavelengths in different locations varies from slightly over 30 m to 130 m, meaning that the optimal dimensions of the OWC chamber can differ significantly by location. However, some regions of the study area must be disregarded when their inherent characteristics exceed the valid application range of the empirical model (see Table 2). These areas are presented in grey in Figure 9.

The optimal OWC chamber geometries for the different geographical locations studied are illustrated in Figure 9 (a). The optimal width of the OWC chamber varies significantly for the different locations, with substantial variations between locations that are relatively close to each other. The west and south coasts of Ireland are an example of these substantial variations within a relatively small area, where the optimal width of the OWC chamber almost doubles with a location further into the ocean. Similarly, the optimal OWC chamber geometry varies signifcantly over relatively short distances along the northwest coast of Africa, with decreasing optimal OWC chamber width towards the south. These differences in optimal geometry are directly related to the differences in wavelength between the analysed locations, as illustrated in Figure 2 (c).

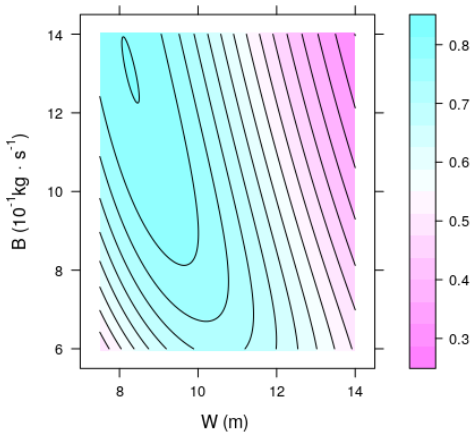

(a) $\lambda = 70$ m

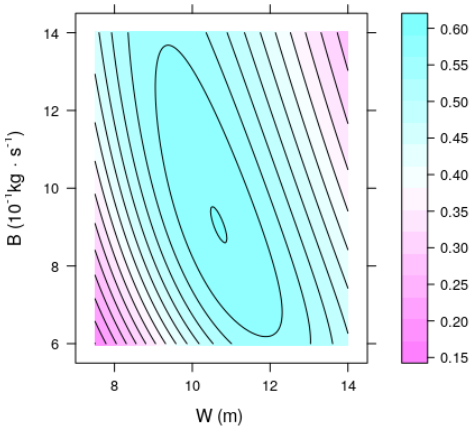

(b) $\lambda = 90$ m

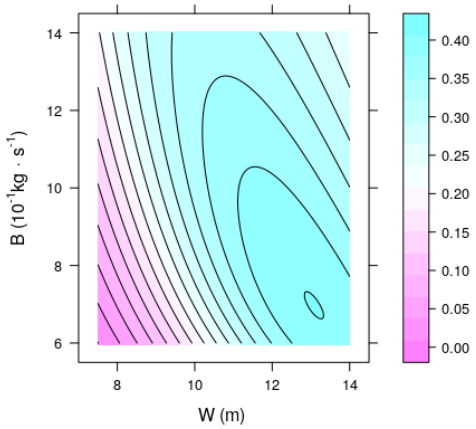

(c) $\lambda = 110$ m

Figure 7: Capture width of the OWC WEC for different chamber dimensions and turbine-induced damping values with a wavelength of (a) 70 m, (b) 90 m, and (c) 110 m.

3.2.2. Impact of Wave Trends

Differences in the optimal geometry of the OWC chamber for different locations have previously been shown in the literature, though not for such a large area of study. However, more importantly than the variations in OWC geometry for different geographical locations, Figure 9 (b)

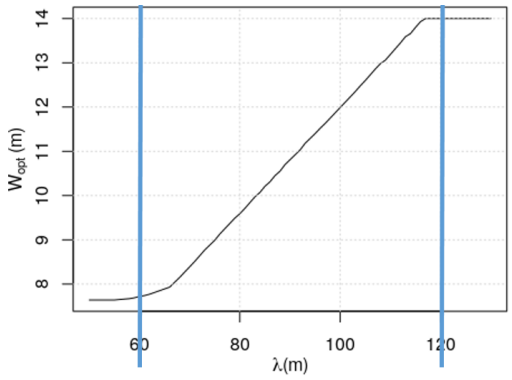

Figure 8: Optimal width W_{opt} of the OWC WEC versus λ. The application range is between 60 m and 120 m.

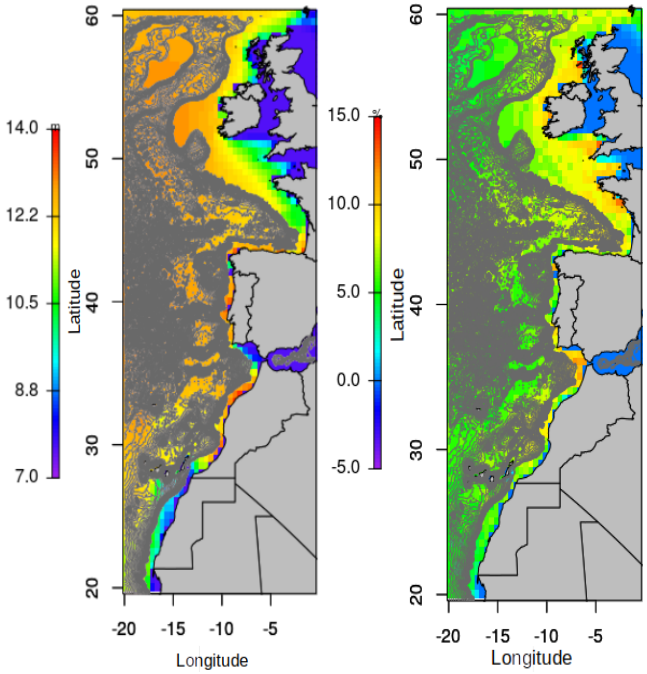

(a) W_{opt} (b) ΔW_{opt}

Figure 9: Optimal OWC chamber width W_{opt} over the area of study based on (a) the average wave resource between 1979 and 2018, and (b) the variation of the optimal width ΔW_{opt} between the decades 1979-88 and 2009-18 in percentage values.

shows the variation in the optimal dimensions of the OWC chamber ΔW_{opt} (as a percentage) between 1979-88 and 2009-18. The wave energy resource varies over time across the geographical study area, which is shown to have a meaningful impact on the optimal OWC chamber geometry. The regions in dark grey also represent deep-water areas that are outside the validity limits of the empirical model.

The increase in W_{opt} from 1979-88 to 2009-18 is the greatest off the west coast of Ireland, Portugal, the Gulf of Biscay and Morocco, showing significant W_{opt} increases of over 10%, with values of up to 15% in Brittany, Galway Bay and certain parts of the Moroccan coast. In con-

trast, the variation of the optimal OWC chamber dimension ΔW_{opt} in sheltered areas, such as the Mediterranean Sea and the coast of Senegal, is negligible. This is consistent with the minimal wave trends observed in the same areas (see Figure 5). This demonstrates that wave trends impact both the energy absorption of WECs and, thus, the geometry of a WEC. Accordingly, a WEC should be specifically designed not only for a given location, but also for a specific period of time—namely, when the WEC is intended to be deployed. However, the true impact of these wave trends should be analysed based on the final energy generation of the various implemented WEC designs.

For example, a WEC that was supposed to be deployed in 1999 with an estimated life of 20 years, would traditionally be designed and optimised based on the past wave energy resource from 1979 to 1998. However, the WEC would actually be deployed in the wave resource between 1999 and 2018; thus, the WEC should be designed for the same period of time. Therefore, evaluating the difference between the two designs (*i.e.* the *original* design based on the resource between 1979-1998 and the *updated* design based on the resource between 1999-2018) is crucial to assess the real impact of wave trends on the design of WECs. Hence, Table 4 shows the optimal width W_{opt} of the *original* design and the absorbed energy (E_{abs}) when the WEC was deployed in 1999 for 20 years. In addition, Table 4 shows the difference between the *updated* and *original* designs ΔW_{opt} in absolute values and the differences between their energy absorption capabilities ΔE_{abs} in relative values.

The energy absorbed by a WEC is proportional to the wave energy flux J_w and is computed considering the CW of the OWC device, which depends on the design of the OWC chamber. In the present case, E_{abs} was calculated using the J_w for the period between 1999-2018 for the *original* and *updated* OWC chamber designs. The monthly values of CW_i and J_{w_i} were thus considered as follows,

$$E_{abs} = \sum_{i=1}^{240} CW_i \cdot J_{w_i} \cdot t_i \tag{11}$$

where 240 is the number of months in 20 years and t_i is the number of hours in each month.

The results shown in Table 4 are especially relevant in Zierbena (*B1*). Due to the substantial variation in λ in this location, it can be seen that the optimal size of the OWC chamber should be extended by 0.7 m (compared to the 10.8 m of the *original* design) for the wave period between 1999-2018. Consequently, the *updated* design would generate 10.8 GWh over the 20 years of operation, which means a 13.5% increase in power output compared to the 9.5 GWh output of the *original* design. For E1 and E2, the difference between the *original* and the *updated* design geometries is lower—approximately 0.4 and 0.2 m, respectively—which would result in a difference in power output of approximately 8% and 6% in E_{abs}.

Table 4: Optimal OWC chamber size for the four locations and the absorbed energy and consequent variations from 1999 to 2018 .

	B1	**B2**	**E1**	**E2**
Original W_{opt}(m)	10.8	12.0	11.4	13.8
Original E_{abs} (GWh)	9.5	16.2	14.6	13.8
ΔW_{opt} (m)	+0.7	-0.8	+0.4	+0.2
ΔE_{abs} (%)	+13.5	0.0	+8.7	+6.5

Finally, the case of B2 in Las Palmas is paradigmatic. The general reduction in wavelength observed at B2 should lead to the design of a smaller *updated* OWC chamber compared to the *original* design. However, this decrease also implies a reduction in the CW (not the CW^*), which would result in the same E_{abs} as the *original* design. Nevertheless, a reduction in size that provides the same amount of absorbed energy is valuable to WEC developers, since the size reduction would likely confer a considerable reduction in WEC production cost.

4. Discussion

Offshore renewable energy devices and farms have conventionally been designed based on the energy resources of the location where the device or farm is to be installed. These energy resources are typically considered as a time-invariant feature in the design process and, as a consequence, the design process of WECs is always based on past wave energy resources. However, long-term variations of the energy resource can be significant within the lifespan of an offshore renewable energy device, which is approximately 25 years. Considering energy resources as time-variant thus has important consequences for crucial aspects of offshore renewable energy systems in general. In particular, for WECs, the design of the device including its geometry, PTO system, and mooring lines, power generation assessment, and the useful life of different components and the system as a whole, among other features, are affected by energy resource variations. Therefore, a precise understanding of long-term wave trends is essential to critically evaluate their impact on WEC systems.

The wave energy potential results and wave trends obtained in this study are consistent with previous results for deep-water regions around Portugal, the Bay of Biscay, and Ireland [50, 51, 52, 53, 34, 28, 35], where wave energy potential varies between 30 and 50 kW/m. However, these wave trends must be analysed in detail to fully understand the physical processes driving these trends. Some studies have suggested that the evolution of wave energy resources is directly related to ocean warming and climate change [54]. Other studies have identified teleconnection patterns and their variations, such as the North Atlantic Oscillation or the Arctic Oscillation, as the main cause of long-term resource variations [36]. Nevertheless, understanding these wave trends, and the climatic patterns and dynamics behind them, is vital to predict future energy

resources to design offshore renewable energy devices accurately and cost-effectively.

The wave energy absorption values obtained in this study are also consistent with previously published studies. The wavelength values measured in the study area correspond to capture width ratios of approximately 0.4-0.6 m. This implies an optimum absorption of 15-25 kW, based on the empirical model proposed in [27]. Similar values were also found in [55], where the the Plant Efficiency Index (PEI) of the Mutriku OWC plant was studied. The PEI index is analogous to the CW, although it considers the final electricity production rather than merely the pneumatic mechanical power absorption, as was considered in the present study and in [46]. As a consequence, the PEI values presented in [55] are slightly lower—approximately 0.3 m for the Mutriku OWC power plant—than the CW values presented in this study.

The levelised cost of energy (LCOE) in $/MWh can also be analysed to evaluate the economic impact of the results obtained in the present study. The LCOE represents the cost of a power generation system over its lifespan. The LCOE of an OWC has been studied in [56] for the Portuguese coast, where the results indicate that the northwestern coast of Portugal is the best location for the installation of wave energy farms with regards to energy cost, with an LCOE of approximately 90 $/MWh. However, the wave trends observed along the northwest coast of Portugal are significant, as shown in Figure 2. Thus, this LCOE value is likely to vary accordingly, and a different location may become a better choice for the installation of a wave energy farm. Alternatively, the design of the WEC device along the Portuguese coast may need to be adapted with the evolution of the wave resource to maintain the current LCOE.

Finally, the results of the present study show the positive impact of considering wave trends in the design of WEC geometry, since the compromise between the size of the structure and the generated energy was shown to be consistently positive. In the case of the B1 location, an increase of approximately 7% in the OWC chamber width results in an increase of over 13% in generated energy. Alternatively, in the case of the B2 location, the same amount of energy can be generated with a significant reduction of approximately 7% in the chamber width. This may have significant implications for the cost of designing and implementing efficient WEC systems.

5. Conclusions

Wave resource variations in the North-East Atlantic Ocean over the last century have been demonstrated in various previous studies, including a significant increase in extreme weather events in some locations. The impact of these resource variations on the performance of WECs has also been described, showing that an increase in the wave energy resource does not necessarily result in increased energy absorption by WECs. This is especially relevant as the frequency of extreme events increases significantly, which can severely damage WECs while reducing extractable wave energy.

However, the impact of wave energy trends on the design of WECs has not been fully explored. This paper presents the first attempt to evaluate the influence of wave trends on the design of the OWC chambers using an empirical model proposed in [27] and created using a vast dataset comprised of experimental and numerical results. This empirical model shows an almost linear relationship between wavelength and the optimal OWC chamber width when keeping the rest of the geometric characteristics constant and optimising turbine damping. This suggests that the optimal chamber width can significantly differ depending on the variation in wave resources.

Wave resource variations were analysed across the North-East Atlantic Ocean, and significant variations were observed between geographical locations and different time periods between 1979 and 2018. As a result, the optimal width of the OWC chamber was shown to vary considerably across the analysed geographical locations and over the studied period of time. Hence, this study demonstrated that optimising the design of a WEC using past wave resource data can result in an inefficient and/or oversized structure. Optimising the design based on the predicted wave resources for when the WEC is intended for deployment can significantly affect the WEC design, resulting in an absorbed energy difference of approximately 15%. Thus, considering the predicted available wave resources may have a positive economic impact on the viability of WECs by increasing their LCOE.

6. Acknowledgments

This research was supported by the University of Basque Country under the contract (UPV/EHU, GIU17/002).

References

[1] IPBES, Summary for policymakers of the global assessment report on biodiversity and ecosystem services, Tech. rep., Intergovernmental Science-Policy Platform on Biodiversity and Ecosystem Services (IPBES) (2019).

[2] IPCC, Global warming of 1.5oc, Tech. Rep. ISBN 978-92-9169-151-7, Intergovernmental Panel on Climate Change (IPCC) (2018).

[3] UNFCCC, Adoption of the paris agreement, Tech. Rep. Report No. FCCC/CP/2015/L.9/Rev.1 (2015).
URL `http://unfccc.int/resource/docs/2015/cop21/eng/l09r01.pdf`

[4] IRENA, Renewable energy: A key climate solution, Tech. Rep. ISBN 978-92-9260-044-0, International Renewable Energy Agency (2017).

[5] M. Z. Jacobson, M. A. Delucchi, Z. A. Bauer, S. C. Goodman, W. E. Chapman, M. A. Cameron, C. Bozonnat, L. Chobadi, H. A. Clonts, P. Enevoldsen, J. R. Erwin, S. N. Fobi, O. K. Goldstrom, E. M. Hennessy, J. Liu, J. Lo, C. B. Meyer, S. B. Morris, K. R. Moy, P. L. ONeill, I. Petkov, S. Redfern, R. Schucker, M. A. Sontag, J. Wang, E. Weiner, A. S. Yachanin, 100% Clean and Renewable Wind, Water, and Sunlight All-Sector Energy Roadmaps for 139 Countries of the World, Joule 1 (1) (2017)

108–121. doi:10.1016/j.joule.2017.07.005.
URL http://dx.doi.org/10.1016/j.joule.2017.07.005

[6] E. Parliament, Directive (eu) 2018/2001 of the european parliament and of the council of 11 december 2018 on the promotion of the use of energy from renewable sources, Tech. Rep. PE/48/2018/REV/1, European Parliament (2018).
URL https://eur-lex.europa.eu/eli/dir/2018/2001/oj

[7] Bloomberg NEF, New energy outlook 2019, Tech. rep. (2019).

[8] Dogger bank wind farms, [Last accessed 09/10/2019].
URL https://doggerbank.com/

[9] A. d. O. Falcao, Wave energy utilization: A review of the technologies, Renewable and sustainable energy reviews 14 (3) (2010) 899–918.

[10] J. Leijon, C. Bostrom, Freshwater production from the motion of ocean waves - a review, Desalination 435 (2018) 161 – 171, desalination using Renewable Energy. doi:https://doi.org/10.1016/j.desal.2017.10.049.
URL http://www.sciencedirect.com/science/article/pii/S0011916417314455

[11] R. J. Bergillos, C. Rodriguez-Delgado, G. Iglesias, Ocean Energy and Coastal Protection, 1st Edition, Springer International Publishing, 2020. doi:10.1007/978-3-030-31318-0.
URL https://www.springer.com/gp/book/9783030313173#aboutAuthors

[12] R. J. Bergillos, C. Rodriguez-Delgado, J. Allen, G. Iglesias, Wave energy converter geometry for coastal flooding mitigation, Science of The Total Environment 668 (2019) 1232 – 1241. doi:https://doi.org/10.1016/j.scitotenv.2019.03.022.
URL http://www.sciencedirect.com/science/article/pii/S0048969719310009

[13] A. Babarit, J. Hals, A. Kurniawan, T. Moan, J. Krokstad, Power absorption measures and comparisons of selected wave energy converters, in: ASME 2011 30th International Conference on Ocean, Offshore and Arctic Engineering, OMAE2011, Vol. 5, 2011, pp. 437–446. doi:10.1115/OMAE2011-49360.

[14] L. Rusu, F. Onea, Assessment of the performances of various wave energy converters along the european continental coasts, Energy 82 (2015) 889 – 904. doi:https://doi.org/10.1016/j.energy.2015.01.099.
URL http://www.sciencedirect.com/science/article/pii/S0360544215001231

[15] M. Penalba, G. Giorgi, J. V. Ringwood, Mathematical modelling of wave energy converters: A review of nonlinear approaches, Renewable and Sustainable Energy Reviews 78 (2017) 1188 – 1207.

[16] G. Giorgi, J. V. Ringwood, A compact 6-dof nonlinear wave energy device model for power assessment and control investigations, IEEE Transactions on Sustainable Energy 10 (1) (2019) 119–126. doi:10.1109/TSTE.2018.2826578.

[17] J. C. Gilloteaux, J. Ringwood, Control-informed geometric optimisation of wave energy converters, IFAC Proceedings Volumes 43 (20) (2010) 366–371. doi:10.3182/20100915-3-DE-3008.00072.

[18] P. B. Garcia-Rosa, J. V. Ringwood, On the sensitivity of optimal wave energy device geometry to the energy maximizing control system, IEEE Transactions on Sustainable Energy 7 (1) (2016) 419–426. doi:10.1109/TSTE.2015.2423551.

[19] A. D. Andres, J. Maillet, J. Hals Todalshaug, P. Möller, H. Jeffreys, On the Optimum Sizing of a Real Wec From a Techno-Economic Perspective, in: Proceedings of the ASME 2016 35th International Conference on Ocean, Offshore and Arctic Engineering, Busan, South Korea, 2016, pp. 1–11.

[20] V. Piscopo, G. Benassai, R. Della Morte, A. Scamardella, Cost-Based Design and Selection of Point Absorber Devices for the Mediterranean Seadoi:10.3390/en11040946.

[21] A. Henry, K. Doherty, L. Cameron, R. Doherty, T. Whittaker, Advances in the design of the oyster wave energy converter, RINA, Royal Institution of Naval Architects - Marine Renewable and Offshore Wind Energy - Papers (January 2015) (2010) 119–128.

[22] P. Schmitt, K. Doherty, T. Whittaker, Shape optimisation of a bottom hinged flap type wave energy converter, in: Proceedings of the Conference on Maritime Energy, 2013.

[23] S. Esmaeilzadeh, M. R. Alam, Shape optimization of wave energy converters for broadband directional incident waves, Ocean Engineering 174 (December 2018) (2019) 186–200. doi:10.1016/j.oceaneng.2019.01.029.
URL https://doi.org/10.1016/j.oceaneng.2019.01.029

[24] A. Garcia-Teruel, D. I. Forehand, Optimal wave energy converter geometry for different modes of motion, in: 3rd International Conference on Renewable Energies Offshore (RENEW), Lisbon, 2018.

[25] B. Bouali, S. Larbi, Contribution to the geometry optimization of an oscillating water column wave energy converter, Energy Procedia 36 (2013) 565 – 573, terraGreen 13 International Conference 2013 - Advancements in Renewable Energy and Clean Environment. doi:https://doi.org/10.1016/j.egypro.2013.07.065.
URL http://www.sciencedirect.com/science/article/pii/S187661021301151X

[26] S. Ribeiro E Silva, R. P. Gomes, A. F. Falcao, Hydrodynamic optimization of the UGEN: Wave energy converter with U-shaped interior oscillating water column, International Journal of Marine Energy 15 (2016) 112–126. doi:10.1016/j.ijome.2016.04.013.
URL http://dx.doi.org/10.1016/j.ijome.2016.04.013

[27] I. Simonetti, L. Cappietti, H. Oumeraci, An empirical model as a supporting tool to optimize the main design parameters of a stationary oscillating water column wave energy converter, Applied Energy 231 (September) (2018) 1205–1215. doi:10.1016/j.apenergy.2018.09.100.
URL https://doi.org/10.1016/j.apenergy.2018.09.100

[28] A. Ulazia, M. Penalba, G. Ibarra-Berastegi, J. Saenz, Wave energy trends over the Bay of Biscay and the consequences for wave energy converters, Energy 141 (C) (2017) 624–634.

[29] M. Penalba, A. Ulazia, G. Ibarra-Berastegui, J. Ringwood, J. Sáenz, Wave energy resource variation off the west coast of Ireland and its impact on realistic wave energy converters' power absorption, Applied Energy 224 (2018) 205 – 219. doi:https://doi.org/10.1016/j.apenergy.2018.04.121.
URL https://www.sciencedirect.com/science/article/pii/S0306261918306895

[30] A. Ulazia, M. Penalba, A. Rabanal, G. Ibarra-Berastegi, J. Ringwood, J. Sáenz, Historical evolution of the wave resource and energy production off the chilean coast over the 20th century, Energies 11 (9) (2018) 2289.

[31] J. Journée, W. W. Massie, Offshore Hydromechanics, first edit Edition, TUDelft, Faculty of Marine Technology, Ship Hydromechanics Laboratory, Delft, The Netherlands, 2001.

[32] C. Stefanakos, et al., Intercomparison of wave reanalysis based on era5 and ww3 databases, in: The 29th International Ocean and Polar Engineering Conference, International Society of Offshore and Polar Engineers, 2019.

[33] P.P.E., Puertos del Estado: Oceanography: Forecast, real time and climate, Spanish Government: Madrid. Updated 2015-10-11. http://www.puertos.es/en-us/oceanografia/Pages/portus.aspx (10 2015).

[34] M. Penalba, A. Ulazia, G. Ibarra-berastegui, J. Ringwood, J. Sáenz, Wave energy resource variation off the west coast of Ireland and its impact on realistic wave energy converters' power absorption, Applied Energy 224 (2018) (2018) 205–219. doi:10.1016/j.apenergy.2018.04.121.

[35] A. Ulazia, M. Penalba, G. Ibarra-Berastegui, J. Ringwood, J. Sáenz, Reduction of the capture width of wave energy converters due to long-term seasonal wave energy trends, Renewable and Sustainable Energy Reviews 113 (2019) 109267. doi:https://doi.org/10.1016/j.rser.2019.109267.
URL http://www.sciencedirect.com/science/article/pii/S1364032119304757

[36] M. Penalba, A. Ulazia, J. Saénz, J. V. Ringwood, Impact of long-term resource variations on wave energy farms: The icelandic case, Energy 192 (2020) 116609.

[37] K. E. Taylor, Summarizing multiple aspects of model performance in a single diagram, Journal of Geophysical Research: Atmospheres 106 (D7) (2001) 7183–7192.
[38] T. V. Heath, A review of oscillating water columns, Philosophical Transactions of the Royal Society A: Mathematical, Physical and Engineering Sciences 370 (1959) (2012) 235–245. doi:10.1098/rsta.2011.0164.
[39] A. F. Falcao, J. C. Henriques, Oscillating-water-column wave energy converters and air turbines: A review, Renewable Energy 85 (2016) 1391 – 1424. doi:https://doi.org/10.1016/j.renene.2015.07.086.
URL http://www.sciencedirect.com/science/article/pii/S0960148115301828
[40] A. Falcao, The shoreline owc wave power plant at the azores, in: Fourth European Wave Energy Conference, Aalborg, Denmark, 2000, pp. 42–47.
[41] T. Heath, T. Whittaker, C. Boake, The design, construction and operation of the limpet wave energy converter (islay, scotland), in: Fourth European Wave Energy Conference, Aalborg, Denmark, 2000, pp. 49–55.
[42] Y. Torre-Enciso, I. Ortubia, L. Lopez de Aguileta, J. Marques, Mutriku wave power plant: from the thinking out to the reality, in: 8th European Wave and Tidal Energy Conference, Uppsala, Sweden, 2009, pp. 319–329.
[43] J. Rea, J. Kelly, R. Alcorn, D. O'Sullivan, Development and operation of a power take-off rig for ocean energy research and testing, in: 9th European Wave and Tidal Energy Conference, Southampton, UK, 2011.
[44] H. Osawa, Y. Washio, T. Ogata, Y. Tsuritani, Y. Nagata, The offshore floating type wave power device mighty whale open sea testsperformance of the prototype, in: International Society of Offshore and Polar Engineers (ISOPE), no. ISOPE-I-02-090, 2002.
[45] A. A. Carrelhas, L. M. Gato, J. C. Henriques, A. F. Falcao, J. Varandas, Test results of a 30?kW self-rectifying bi-radial air turbine-generator prototype, Renewable and Sustainable Energy Reviews 109 (August 2018) (2019) 187–198. doi:10.1016/j.rser.2019.04.008.
URL https://doi.org/10.1016/j.rser.2019.04.008
[46] A. Babarit, A database of capture width ratio of wave energy converters, Renewable Energy 80 (2015) 610–628. doi:10.1016/j.renene.2015.02.049.
[47] I. Crema, I. Simonetti, L. Cappietti, H. Oumeraci, Laboratory Experiments on Oscillating Water Column Wave Energy Converters Integrated in a Very Large Floating Structure, 11th European Wave and Tidal Energy Conference, EWTEC 2015 (September) (2015).
URL https://www.researchgate.net/publication/281900091
[48] I. Simonetti, L. Cappietti, H. Elsafti, H. Oumeraci, Optimization of the geometry and the turbine induced damping for fixed detached and asymmetric owc devices: A numerical study, Energy 139 (2017) 1197 – 1209. doi:https://doi.org/10.1016/j.energy.2017.08.033.
URL http://www.sciencedirect.com/science/article/pii/S0360544217314111
[49] H. Theil, A rank-invariant method of linear and polynomial regression analysis, 3; confidence regions for the parameters of polynomial regression equations, Stichting Mathematisch Centrum. Statistische Afdeling (1950) 1–16.
[50] E. Rusu, Numerical modeling of the wave energy propagation in the iberian nearshore, Energies 11 (4) (2018) 980.
[51] F. Onea, E. Rusu, Sustainability of the reanalysis databases in predicting the wind and wave power along the european coasts, Sustainability 10 (1) (2018) 193.
[52] F. Onea, E. Rusu, The expected efficiency and coastal impact of a hybrid energy farm operating in the portuguese nearshore, Energy 97 (2016) 411–423.
[53] E. Rusu, F. Onea, Estimation of the wave energy conversion efficiency in the atlantic ocean close to the european islands, Renewable Energy 85 (2016) 687–703.
[54] B. G. Reguero, I. J. Losada, F. J. Méndez, A recent increase in global wave power as a consequence of oceanic warming, Nature communications 10 (2019).
[55] G. Ibarra-Berastegi, J. Sáenz, A. Ulazia, P. Serras, G. Esnaola, C. Garcia-Soto, Electricity production, capacity factor, and plant efficiency index at the mutriku wave farm (2014–2016), Ocean Engineering 147 (2018) 20–29.
[56] L. Castro-Santos, G. P. Garcia, A. Estanqueiro, P. A. Justino, The levelized cost of energy (lcoe) of wave energy using gis based analysis: The case study of portugal, International Journal of Electrical Power & Energy Systems 65 (2015) 21–25.